Limit Cycles in Homogeneous Azeotropic Distillation

Moonyong Lee,† Cornelius Dorn, George A. Meski,‡ and Manfred Morari*

Automatic Control Laboratory, ETH-Z, Swiss Federal Institute of Technology, CH-8092 Zürich, Switzerland

In spite of significant nonlinearities even in the simplest model, the distillation literature generally takes for granted that distillation columns display relatively simple dynamic behavior. For example, although widely observed in chemical reactors, any instances of periodic oscillations have not yet been associated with models of distillation columns. In this paper we study the steady-state and dynamic behavior of the azeotropic distillation of the ternary homogeneous system methanol−methyl butyrate−toluene. Our simulations reveal nonlinear behavior not reported in earlier studies. Under certain conditions, the open-loop distillation system shows a sustained oscillation (limit cycle). The limit cycles are accompanied by traveling waves inside the column. Significant underdamped oscillations are also observed over a wide range of product rates. To our knowledge, this is the first simulation result reporting the presence of Hopf bifurcation points in open-loop distillation models.

1. Introduction

Azeotropic distillation is one of the most widely used and important separation processes in the chemical and the specialty chemical industries. Because their understanding is a necessary prerequisite for proper column design and operation, the steady-state and dynamic behavior of azeotropic distillation has been studied extensively over the past decades. Laroche et al.[1] have shown that azeotropic distillation columns can exhibit unusual features not observed in nonazeotropic distillation. In particular, multiplicity of steady states has been a subject of much recent research interest. An overview of steady-state multiplicity in distillation is given by Güttinger et al.[2]

By multiple steady states in a column we mean the general notion of multiplicities, i.e., that a system with as many parameters specified as there are degrees of freedom exhibits different solutions at steady state. In this paper, the term "multiple steady states" (MSS) refers to output multiplicities only. Throughout this work, only multiplicities of type II[2] will be considered. Multiplicities of this type are caused by the vapor−liquid equilibrium (VLE) as well as the complex recycle structure between the stages. They can be predicted from minimal data with the ∞/∞ analysis[3] (first proposed by Petlyuk and Avetyan[4]). Multiplicities of type II have been verified experimentally[2,5,6] and are now widely accepted. In addition to multiple steady states, another well-known phenomenon which nonlinear systems can exhibit is sustained oscillations (limit cycles). However, in spite of significant nonlinearities in the distillation models, all asymptotic solutions discovered so far are stationary. Until now, no periodic solution has been associated with any class of open-loop column models while it has been well recognized in the chemical reactor literature for several decades. In this context, "open-loop" means that only the pressure and level control loops are closed under perfect control. The evidence of other behavior such as underdamped oscillation has also been rare whereas it commonly occurs in other nonlinear systems.

Doherty and Perkins[7] showed that in binary, equilibrium-stage distillation (with Murphree efficiencies) all eigenvalues of the Jacobian matrix associated with a constant molar overflow (CMO) model are distinct, real, and negative for all values of the state vector and for all feasible parameter values. In conjunction with the proof by Rosenbrock[8] that the steady state of such column models is unique and globally stable, it follows that no sustained oscillations are possible in this case. However, for less simplified models or for mixtures with more than two components, the eigenvalues of the Jacobian matrix could be complex. For example, Levy et al.[9] found pairs of complex eigenvalues in a model of a binary distillation column where changes in composition, enthalpy (energy balances), and holdup were taken into account. Analysis of the eigenvectors corresponding to the complex eigenvalues revealed that they had predominantly hydraulic terms.

To our knowledge, the first dynamic simulation results showing underdamped oscillation in heterogeneous distillation were published by Widagdo et al.[10] They simulated the dehydration of *sec*-butanol with di-*sec*-butyl ether in a 12-tray column with decanter. Rigorous vapor−liquid−liquid calculations were included for all trays and the decanter.

Recently, some oscillatory behavior has been observed in experiments. Sundmacher and Hoffmann[11] reported sustained oscillations in a packed reactive column for MTBE production as well as for nonreactive distillation of methanol and isobutene. Wang et al.[12] observed oscillatory behavior in a pilot-scale column for the azeotropic distillation of cyclohexane−isopropyl alcohol−water. However, the accompanying dynamic simulations did not reproduce the oscillations. Thus, it is unclear whether the oscillations observed were caused by system nonlinearities in the vapor−liquid equilibrium or just by unmeasured control actions and peculiarities in the experimental setup. Because of the results of Doherty

* Author to whom correspondence should be addressed. Phone: +41 1 632-2271. Fax: +41 1 632-1211. E-mail: morari@aut.ee.ethz.ch.

† Current address: School of Chemical Engineering and Technology, Yeungnam University, Dae-Dong 214-1, Korea.

‡ Current address: A23D3, MIS/RES, Air Products and Chemicals, 7201 Hamilton Boulevard, Allentown, PA 18195-1501.

10.1021/ie980093h CCC: $18.00
Published on Web 03/26/1999

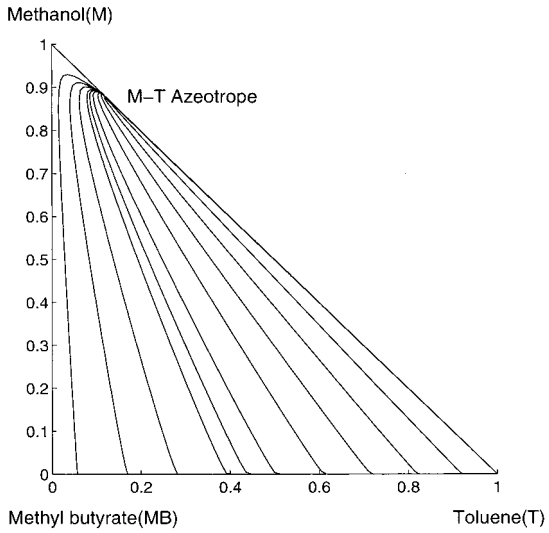

Figure 1. Residue curve diagram (mole fractions) of the ternary mixture methanol (M)−methyl butyrate (MB)−toluene (T) at p = 1 atm.

and Perkins,[7] the oscillations in the binary distillation of methanol and isobutene reported by Sundmacher and Hoffmann[11] cannot be caused by the vapor−liquid equilibrium alone as the Jacobian matrix of the corresponding CMO model has no complex eigenvalues. Simulations by Jacobsen and Skogestad[13] demonstrated Hopf bifurcations and limit cycles in the distillation of methanol and propanol. However, those were caused by interactions of the level controllers and the column.

In light of these discussions, it is natural to ask whether open-loop distillation is able to exhibit periodic solutions (Hopf bifurcation).

In this paper, the presence of periodic solutions in an open-loop distillation model is demonstrated through the simulation of the azeotropic distillation of methanol−methyl butyrate−toluene. In the next section, we describe the dynamic model used in the simulations. Finally, we present results of the nonlinear dynamic simulations and the bifurcation analysis of the column.

2. Simulation Setup

2.1. Mixture. The ternary homogeneous mixture methanol (M)−methyl butyrate (MB)−toluene (T) used in the experimental study by Güttinger et al.[2] is chosen here. The mixture belongs to the class 001 according to Matsuyama and Nishimura.[14] The residue curve diagram for the mixture is given in Figure 1. The binary minimum-boiling M−T azeotrope is located at 88 mol % methanol.

2.2. CMO Model. In order to focus on the nonlinear behavior caused by the vapor−liquid equilibrium, a CMO model is used. Several assumptions are made in the model including (1) constant molar overflow (neglect energy balances), (2) constant molar liquid holdup on the trays, the condenser, and reboiler, (3) negligible vapor holdup, (4) total condenser without subcooling, (5) saturated liquid feed, (6) constant column pressure and no pressure drop between trays, and (7) a Murphree tray efficiency of 1.

The vapor phase is assumed to be ideal, and the vapor pressures are calculated with the Antoine equation. The liquid activity coefficients are computed using the Wilson model. The thermodynamic parameters are taken from Güttinger et al.[2]

Table 1. Column Data for Simulation (CMO Model)

no. of trays (including condenser and reboiler)	46
feed tray (counting from condenser)	41
tray liquid holdup (kmol)	3
condenser liquid holdup (kmol)	3
reboiler liquid holdup (kmol)	3
column pressure (atm)	1.0
reflux flow rate (kmol/h)	1200
feed flow rate (kmol/h)	100
feed composition methanol (mole fraction)	0.8671
feed composition methyl butyrate (mole fraction)	0.0050
feed composition toluene (mole fraction)	0.1279

For the dynamic simulations, the CMO model is integrated using DDASAC.[15] AUTO[16] is used for a steady-state bifurcation analysis of the CMO model. To investigate the local dynamic behavior and stability, the eigenvalues are calculated with LAPACK[17] by linearizing the nonlinear CMO model at every steady state.

Data for the simulation are given in Table 1. The trays are counted from the condenser down. Because of the delicate nature of the dynamic problem under study, special attention was paid to numerical computation; all of the routines used were in double precision with sufficiently tight tolerances.

In all simulations, compositions and flow rates are specified on a "molar" basis so that any effect due to the nonlinear relationship between the mass and molar flow rates[18] is excluded.

3. Simulation Results

3.1. ∞/∞ Prediction and Steady-State Simulation. First, the ∞/∞ analysis was applied for a quick preliminary bifurcation analysis. From the ∞/∞ analysis, it is conjectured that for the given system class the maximum product flow rate range for multiplicity is reached as the feed composition tends to the binary M−T azeotrope. Thus, the feed composition (see Table 1) was chosen such that a large multiplicity range would exist.

The bifurcation diagrams predicted by the ∞/∞ analysis are shown in Figures 2 and 3 (solid lines). The distillate flow rate was used as the bifurcation parameter. In the same figures, the steady-state solution branches calculated with the CMO model are given. Because the column is operated at finite reflux and has a finite number of trays, there are some quantitative differences between the ∞/∞ predictions and the simulations with the CMO model (specifically, close to one of the turning points). However, the results are in good qualitative agreement.

3.2. Bifurcation Analysis and Dynamic Simulations. Figure 4 shows the bifurcation diagram based on the computations from AUTO and eigenvalue calculations. For the bifurcation diagram, the weighted average temperature of all trays, the reboiler, and the condenser is chosen as a scalar index for the state variables of the column:

$$T^{\mathrm{avg}}(t) = \frac{\sum_{j=1}^{N} T^j(t)\, M^j}{\sum_{j=1}^{N} M^j}$$

This quantity was chosen to provide some engineering

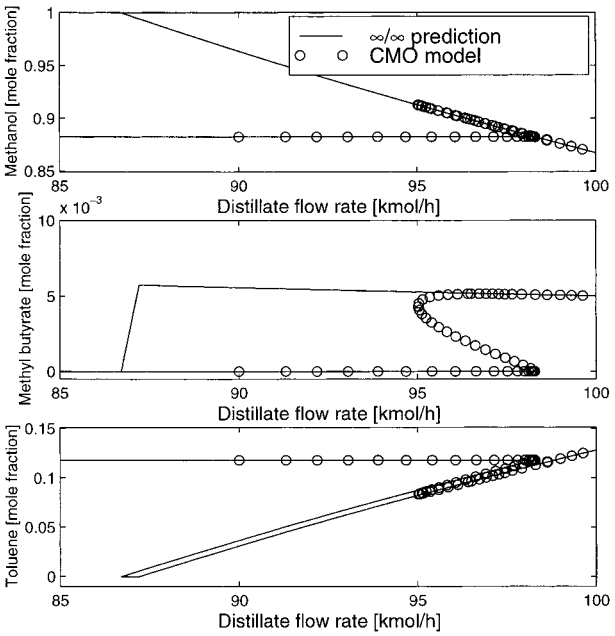

Figure 2. Steady-state bifurcation diagram showing the distillate compositions as a function of the distillate flow rate.

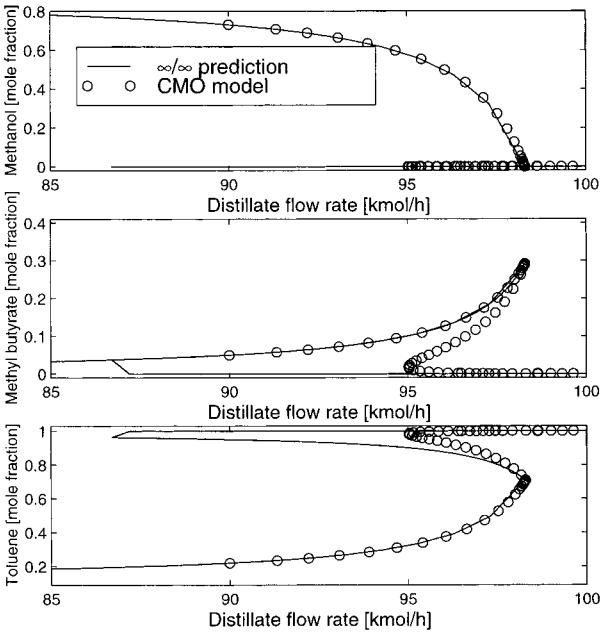

Figure 3. Steady-state bifurcation diagram showing the bottom compositions as a function of the distillate flow rate.

insight. Obviously, any other state variable could have been used. In Figure 4 one can see two turning points (L_1 and L_2) which accompany multiple solutions. This type of bifurcation is well recognized in distillation. An interesting new type of bifurcation observed here is the Hopf bifurcation. The upper branch bifurcates to limit cycles for $D/F \in (0.9641, 0.9735)$. The limit cycles are plotted as solid dots in Figure 4. The distance of the dots from the steady-state branch depicts half of the difference between the maximum and minimum average temperatures during the sustained oscillation and thus indicates the "amplitude" of the limit cycle.

Let us now proceed to a detailed discussion of the dynamic behavior as D/F is varied from 0 to 1. The qualitatively different kinds of dynamic behaviors caused by the existence of one or three steady states which can be stable or unstable nodes, saddles, foci, etc., are

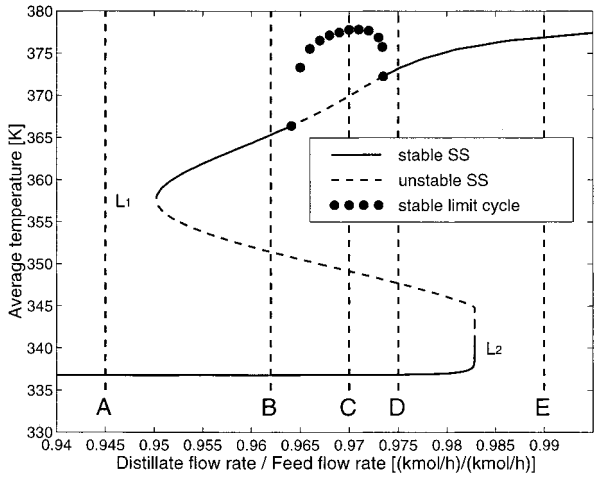

Figure 4. Steady-state bifurcation showing the average temperature in the column (CMO model).

illustrated with dynamic simulations. For selected values of the bifurcation parameter, nonlinear dynamic simulations were carried out starting from different unsteady initial conditions. The average liquid composition in the column

$$x_c^{avg}(t) = \frac{\sum_{j=1}^{N} x_c^j(t)\, M^j}{\sum_{j=1}^{N} M^j}$$

during each simulation is plotted in the composition space in Figure 5a−e. The average liquid composition x_c^{avg} is a normalized measure of the column inventory of component c.

***D/F* < 0.9502: One Steady State.** For values of D/F to the left of the turning point L_1, only a single stable steady state exists. Figure 5a shows selected phase plane trajectories for $D/F = 0.945$. The column has a single stable node (no oscillation) in this particular case.

0.9502 < *D/F* < 0.9641: Three Steady States (Oscillations). In this part of the region of multiplicity, the steady states on the low and high branch are stable and those on the intermediate branch are unstable. As illustrated in Figure 5b for $D/F = 0.9620$, the trajectories converge to either the stable node or the stable focus. The stable node corresponds to the steady state on the low branch. An interesting observation is the appearance of the focus corresponding to the stable steady state on the high branch which has been rarely observed in open-loop distillation.

0.9641 < *D/F* < 0.9735: Three Steady States (Limit Cycle). For values of the bifurcation parameter in this region, branching to periodic solutions occurs, the steady state on the upper branch becomes unstable, and a limit cycle grows around it. Therefore, two types of attractors exist for values of D/F in this region: a stable node and a limit cycle. Figure 5c illustrates a phase plot corresponding to this case. A pronounced stable limit cycle surrounds the unstable steady state on the high branch. The bifurcation is supercritical in this case as the resulting limit cycle is stable.

Figure 6 shows the time domain responses of the average liquid composition in the column to a small perturbation in D starting from the unstable steady

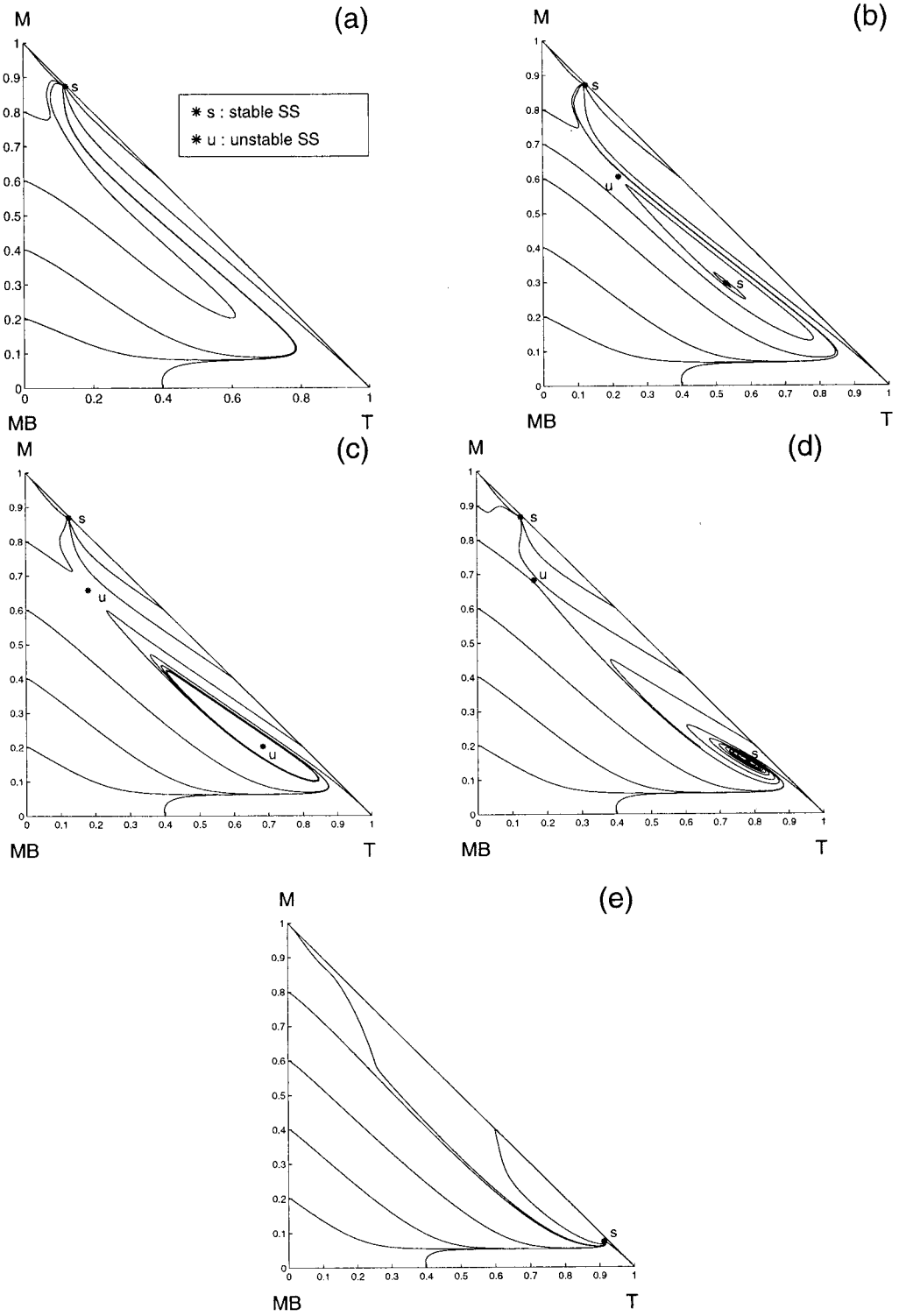

Figure 5. Phase diagrams of the average liquid composition in the column (corresponding to different regions in Figure 4). D/F = (a) 0.945, (b) 0.962, (c) 0.97, (d) 0.974, and (e) 0.99.

state on the high branch for $D/F = 0.9700$. The period of oscillation is ≈110 h. The instability and limit cycle related to the Hopf bifurcation also appear in each state variable of the column with various nonlinear patterns. Figure 7 illustrates the phase plane response of the actual liquid composition on tray 12. The variables eventually reach a limit cycle with asymmetric shape. Figure 8 shows the corresponding time domain responses of temperature and liquid composition on tray 12. The response of the methyl butyrate fraction shows a periodicity with a double peak as expected from the sickle shape of the limit cycle in Figure 7. During each period of the oscillation, the composition varies significantly, e.g., the methanol mole fraction between 0.002 and 0.9606. In Figure 9, the movement of the temperature front inside the column during the oscillation is given at intervals of $\Delta t = 10$ h. Note that the velocity and shape of the front moving up and down are different.

0.9735 < *D/F* < 0.9828: Three Steady States (Oscillations). In this region, the limit cycle disappears and the steady state on the high branch is stable again.

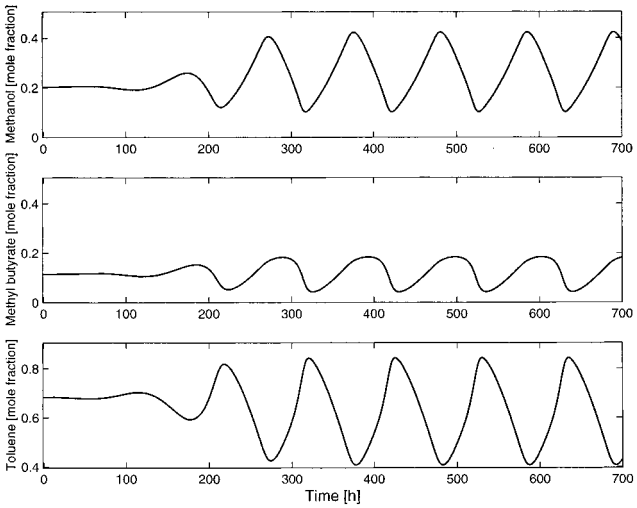

Figure 6. Response of average liquid composition in the column starting at an unstable steady state on the high branch for $D/F = 0.97$ (see also Figure 5c).

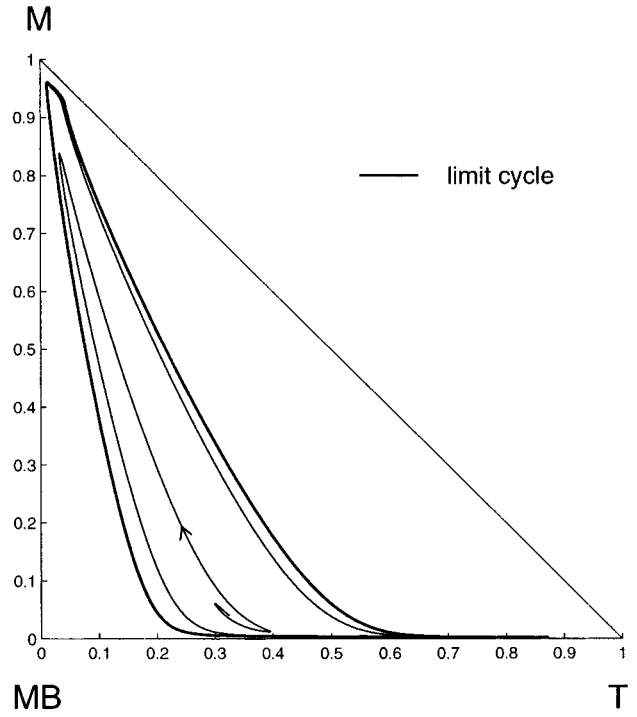

Figure 7. Phase plot of liquid composition on tray 12 starting at an unstable steady state on the high branch for $D/F = 0.97$ (see also Figure 5c).

Phase plane trajectories for this case are shown in Figure 5d. Three steady states exist: one stable node, one saddle, and one stable focus. The phase pattern is qualitatively the same as that in Figure 5b, but in this case the column shows more severe oscillatory behavior with a larger region of attraction around the stable focus.

Figure 10 shows the time responses of selected tray temperatures when the distillate flow rate is decreased from steady-state operation at $D/F = 0.9760$ to 0.9740 kmol/h at $t = 0$. The oscillation also appears in the temperature profiles: The temperature front of the column approaches the steady-state position in an oscillatory manner (not illustrated).

$0.9828 < D/F$: One Steady State. For values of D/F to the right of the turning point L_2, only one stable steady state exists on the high branch. It is observed

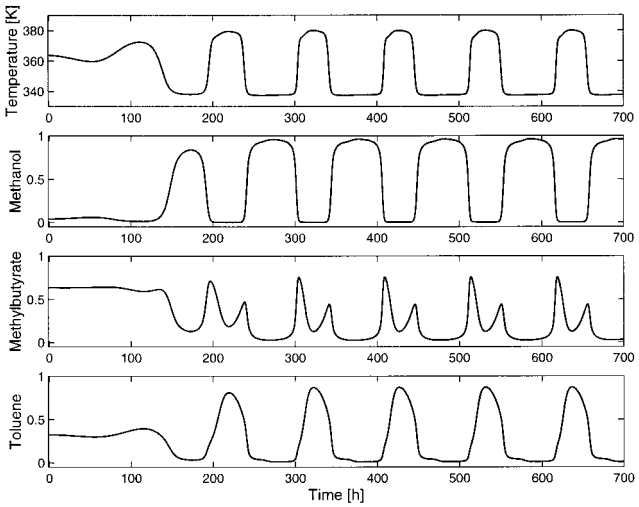

Figure 8. Responses of temperature and liquid mole fractions on tray 12 starting at an unstable steady state on the high branch for $D/F = 0.97$ (see also Figure 5c) (CMO model, Wilson).

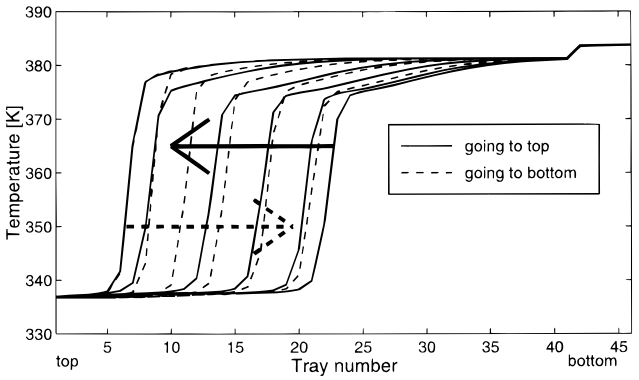

Figure 9. Temperature profiles ($\Delta t = 10$ h) during the sustained oscillation (see also Figure 5c).

that the underdamped oscillatory phenomena continue somewhat after the bifurcation parameter is increased to values outside the region of multiplicity and finally disappear. Figure 5e illustrates the phase trajectories when $D/F = 0.9900$. Only one steady state exists in the form of a stable node.

4. Confirmation with Other Models

In this section the results obtained with the CMO model in section 3 will be reconfirmed with a more complex model.

4.1. Column Model: RADFRAC. The simulation packages Aspen PLUS V.10 and Aspen Dynamics V.10 by Aspen Technology, Inc., were used to reproduce the steady-state bifurcation and the dynamic simulations, respectively. RADFRAC, the distillation column model included in these packages, is a model that includes mass and energy balances, volumetric holdups, rigorous pressure drop calculations, level control for reboiler and condenser, pressure control, etc. For many purposes, this model can be called "rigorous" in comparison to the "simple" CMO model. Compared with the CMO model, most of the design parameters like number of trays, feed composition, etc., were left unchanged. Other parameters that do not exist in the simple model like volumetric holdups were chosen in a way to give a meaningful approximation of the CMO case. (The files needed to do the Aspen simulations can be made available upon

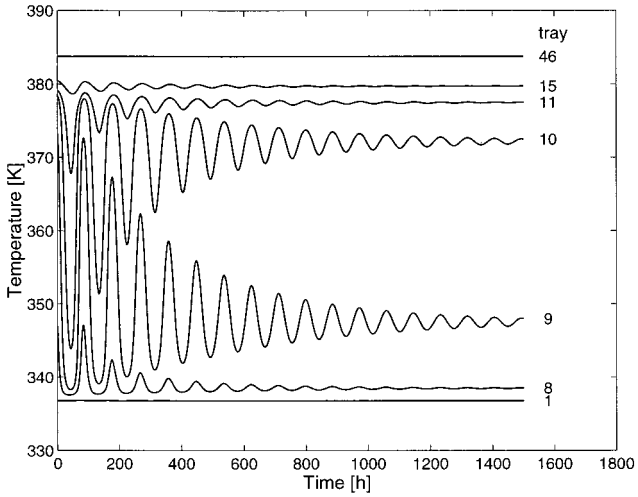

Figure 10. Responses of the tray temperatures to the step decrease in D from $D/F = 0.976$ to 0.974.

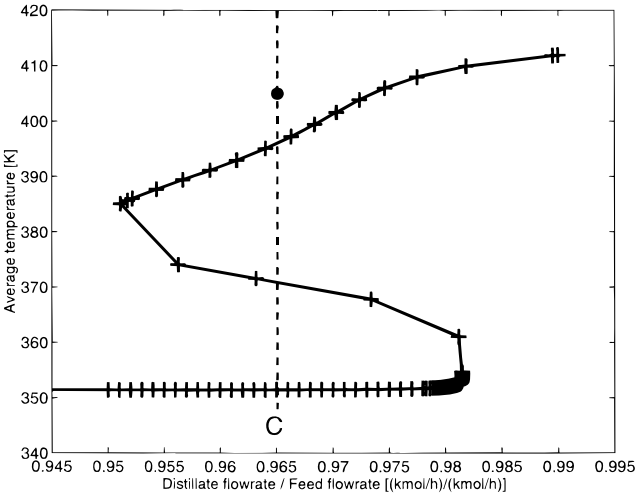

Figure 11. Steady-state bifurcation showing the average temperature in the column (Aspen PLUS, Wilson).

request. Please contact the authors.) However, one change needs to be pointed out: the molar reflux flow rate was increased from $L/F = 12$ to 20. Without this increase of the reflux, only underdamped but no sustained oscillations were observed.

In Figure 11, the bifurcation diagram is shown that corresponds to the diagram shown in Figure 4. Qualitatively, the two are in good agreement. The quantitative differences are due to differences in the models. For example, the rigorous pressure drop calculations result in higher pressures at the bottom of the column compared to the constant pressure assumed in the CMO model. Thus, the boiling temperatures are higher.

Because the stability of steady states cannot be determined in Aspen PLUS, the regions A−E corresponding to those in Figure 4 could not be constructed. Thus, stability could only be studied through dynamic simulation. Here, only one case for region C (limit cycles) will be shown.

In Figure 12, the temperature and liquid composition on tray 12 are shown after the column was initialized on steady state C ($D/F = 0.9651$) on the high branch and a small disturbance on the distillate flow rate was imposed. Qualitatively, the transient is in very good agreement with the transient shown in Figure 8 obtained with the CMO model. Differences such as the

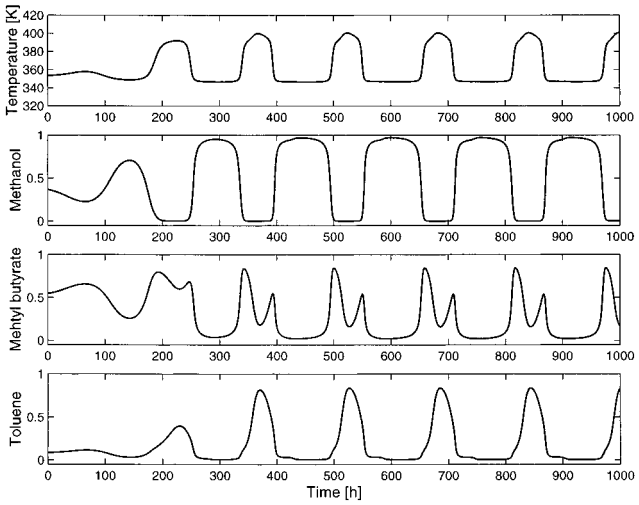

Figure 12. Responses of temperature and liquid mole fractions on tray 12 starting at an unstable steady state on the high branch for $D/F = 0.9651$ (Aspen Dynamics, Wilson).

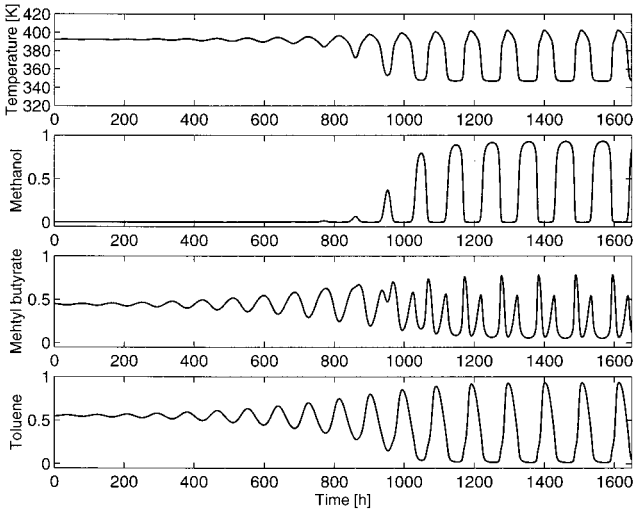

Figure 13. Responses of temperature and liquid mole fractions on tray 12 starting at an unstable steady state on the high branch for $D/F = 0.9571$ (Aspen Dynamics, UNIQUAC).

longer period of oscillation are due to differences in the model, for example, the nonconstant *molar* holdups, which result from the fact that in Aspen Dynamics the trays have constant *volumetric* holdups.

4.2. VLE Model: UNIQUAC. The simulations described in the last subsection were repeated with the Aspen models but using UNIQUAC instead of Wilson as the VLE model. Again, the column was initialized on a steady state ($D/F = 0.9651$) on the high branch in the region C where limit cycles occur, and a small disturbance on the distillate flow rate was imposed. Figure 13 shows the temperature and liquid composition on tray 12. Compared to Figures 8 and 12, which were calculated using the Wilson model for the VLE, the good qualitative agreement is obvious. Differences between Figures 12 and 13 are due to the fact that the binary interaction parameters for the two models were not tuned for "a good match". Instead, the Wilson parameters were taken from work by Güttinger et al.[2] while the UNIQUAC parameters were taken from the Aspen databanks (methanol−toluene) or estimated from UNIFAC (methanol−methyl butyrate, toluene−methyl butyrate).

5. Conclusions

In this paper, we study the dynamic behavior of a ternary homogeneous azeotropic distillation column with the CMO model. Our computations reveal several interesting nonlinear phenomena not reported in previous studies of distillation: a Hopf bifurcation is found. Thus, the column exhibits periodic oscillations over the corresponding region. The sustained oscillations result in periodic movements of the profiles inside the column. The column also shows significant underdamped responses over a wide range of conditions. The results obtained with the CMO model were reconfirmed with a more complex model as well as a different VLE model.

Acknowledgment

Financial support from KOSEF is gratefully acknowledged. The authors thank Thomas E. Güttinger, who programmed the CMO distillation column model used for the simulations.

Notation

F = molar feed flow rate
D = molar distillate flow rate
L = molar reflux flow rate
x_c^j = molar liquid fraction of component c on tray j
T^j = temperature on tray j
M^j = molar liquid holdup on tray j
N = number of trays

Literature Cited

(1) Laroche, L.; Bekiaris, N.; Andersen, H. W.; Morari, M. The Curious Behavior of Homogeneous Azeotropic Distillation—Implications for Entrainer Selection. *AIChE J*. **1992b**, *38* (9), 1309.

(2) Güttinger, T. E.; Dorn, C.; Morari, M. Experimental Study of Multiple Steady States in Homogeneous Azeotropic Distillation. *Ind. Eng. Chem. Res.* **1997**, *36* (3), 794.

(3) Bekiaris, N.; Meski, G. A.; Radu, C. M.; Morari, M. Multiple Steady States in Homogeneous Azeotropic Distillation. *Ind. Eng. Chem. Res.* **1993**, *32* (9), 2023.

(4) Petlyuk, F. B.; Avetyan, V. S. Investigation of Three Component Distillation at Infinite Reflux (in Russian). *Theor. Found. Chem. Eng.* **1971**, *5* (4), 499.

(5) Dorn, C.; Güttinger, T. E.; Wells, G. J.; Morari, M.; Kienle, A.; Klein, E.; Gilles, E.-D. Stabilization of an Unstable Distillation Column. *Ind. Eng. Chem. Res.* **1998**, *37* (2), 506.

(6) Müller, D.; Marquardt, W. Experimental Verification of Multiple Steady States in Heterogeneous Azeotropic Distillation. *Ind. Eng. Chem. Res.* **1997**, *36* (12), 5410.

(7) Doherty, M. F.; Perkins, J. D. On the Dynamics of Distillation Processes IV: Uniqueness and Stability of the Steady State in Homogeneous Continuous Distillations. *Chem. Eng. Sci.* **1982**, *37*, 381.

(8) Rosenbrock, H. H. A Lyapunov Function with Applications to Some Nonlinear Physical Systems. *Automatica* **1962**, *1*, 31.

(9) Levy, R. E.; Foss, A. S.; Grens, E. A. Response Modes of a Binary Distillation Column. *Ind. Eng. Chem. Fundam.* **1969**, *8*, 765.

(10) Widagdo, S.; Seider, W. D.; Sebastian, D. H. Dynamic Analysis of Heterogeneous Azeotropic Distillation. *AIChE J*. **1992**, *38* (8), 1229.

(11) Sundmacher, K.; Hoffmann, U. Oscillatory Vapor−Liquid Transport Phenomena in a Packed Reactive Distillation Column for Fuel Ether Production. *Chem. Eng. J*. **1995**, *57*, 219.

(12) Wang, C. J.; Wong, D. S. H.; Chien, I.-L.; Shih, R. F.; Wang, S. J.; Tsai, C. S. Experimental Investigation of Multiple Steady States and Parametric Sensitivity in Azeotropic Distillation. *Comput. Chem. Eng.* **1997**, *21*, Supplement S535.

(13) Jacobsen, E. W.; Skogestad, S. Instability of Distillation Columns. *AIChE J*. **1994**, *40* (9), 1466.

(14) Matsuyama, H.; Nishimura, H. Topological and Thermodynamic Classification of Ternary Vapor−Liquid Equilibria. *J. Chem. Eng. Jpn*. **1977**, *10* (3), 181.

(15) Stewart, W. E.; Caracotsios, M.; Sorensen, J. P. DDASAC Software Package Documentation, University of Wisconsin, Madison, WI, 1995.

(16) Doedel, E. J.; Champneys, A. R.; Fairgrieve, T. F.; Kuznetsov, Y. A.; Standstede, B.; Wang, X. *AUTO97: Continuation and Bifurcation Software for Ordinary Differential Equations*; Concordia University: Montreal, Canada, 1997; software documentation.

(17) Anderson, E.; Bai, Z.; Bischof, C.; Demmel, J.; Dongarra, J. *Lapack Users' Guide*: Release 2.0; International Society for Industrial and Applied Mathematics, 1995.

(18) Jacobsen, E. W.; Skogestad, S. Multiple Steady States in Ideal Two-Product Distillation. *AIChE J*. **1991**, *37* (4), 499.

Received for review February 16, 1998
Revised manuscript received January 11, 1999
Accepted January 12, 1999

IE980093H